Asian Journal of Chemistry; Vol. 38, No. 2 (2026), 323-333
ASIAN JOURNAL OF CHEMISTRY
https://doi.org/10.14233/ajchem.2026.34912

Eco-Friendly Synthesis, Characterization and Multifunctional Bioactivity of Phyto-Capped Zinc Oxide Nanoparticles Derived from *Kalanchoe fedtschenkoi*

HRISHIKESH H. KHODADE[1,2], DEEPAK B. SHELKE[3,*], HIRALAL B. SONAWANE[1,*], KAMLAKAR C. MORE[4] and MAHADEV R. CHAMBHARE[3]

[1]P.G. Research Centre in Botany, PDEA's Prof. Ramkrishna More ACS College (Affiliated to Savitribai Phule Pune University), Pune-411044, India
[2]Department of Botany, Sharadchandra Pawar Mahavidyalaya, Lonand-415521, India
[3]Department of Botany, Amruteshwar Art's, Commerce and Science College, Vinzar, Velha, Pune-412213, India
[4]Department of Botany, Sant Gadge Baba Amravati University, Amravati-444602, India

*Corresponding authors: E-mail: dpk.shelke1@gmail.com; amolsbr@gmail.com

Received: 17 September 2025 *Accepted*: 12 December 2025 *Published online*: 31 January 2026 AJC-22250

This work reports an eco-friendly approach of synthesis of zinc oxide nanoparticles (Kf-ZnNPs) using leaf extract from *Kalanchoe fedtschenkoi* and evaluates their physico-chemical characteristics along with a broad spectrum of biological activities. The UV-Visible spectroscopy confirmed the formation and optical stability of the nanoparticles through a distinct absorption peak at 349 nm, indicative of monodispersity. Dynamic light scattering and zeta potential analyses revealed a narrow particle size distribution with an average hydrodynamic diameter of approximately 34.20 nm (PDI: 0.001-0.306) and moderate colloidal stability (-11.66 mV). Scanning electron microscopy (SEM) further demonstrated a quasi-spherical morphology with particle sizes ranging between 13.49 and 24.28 nm. FTIR analysis confirmed the involvement of proteins, phenolics and other phytochemicals from the plant extract in nanoparticle reduction and stabilization. The crystalline nature of the nanoparticles was established by X-ray diffraction, which showed a characteristic wurtzite ZnO phase with crystallite sizes between 17.7 to 26.4 nm and an average crystallite size of 21.78 ± 3.42 nm. Biological results revealed the remarkable antibacterial activity of Kf-ZnNPs against *Staphylococcus aureus* and *Escherichia coli*, with inhibition zones of 25 ± 1.00 mm and 22 ± 1.00 mm, respectively, along with significant antifungal efficacy against *Candida albicans* (23 ± 1.00 mm). The nanoparticles also exhibited significant antioxidant, anti-inflammatory and antidiabetic activities, with IC_{50} values of 92 µg/mL, 70.98 µg/mL and 97.13 µg/mL, respectively. Furthermore, the cytotoxicity assays demonstrated substantial anticancer potential against MCF-7 and A549 cell lines, with IC_{50} values of 15 µg/mL and 20.15 µg/mL, respectively.

Keywords: Biological activities, *Kalanchoe fedtschenkoi*, Zinc oxide nanoparticles.

INTRODUCTION

The synthesis of nanoparticles has traditionally relied on a range of physical and chemical techniques, including ball milling, laser ablation, chemical reduction, hydrothermal processing and sol-gel methods. While these approaches offer precise control over particle size and crystallinity, they often demand substantial energy input, specialized instrumentation and hazardous chemical reagents [1-3]. Such requirements not only increase production costs but also raise concerns regarding environmental sustainability and biological safety, particularly in applications related to nanomedicine and biomedical engineering [4].

In response to these challenges, green synthesis strategies have gained significant attention over the past two decades as sustainable alternatives that integrate nanotechnology with principles of environmental compatibility and resource efficiency [5,6]. These approaches utilize biological systems to facilitate the reduction and stabilization of metal ions, thereby minimizing the use of toxic chemicals and aligning with green chemistry concepts [7,8]. Early green synthesis efforts primarily employed microorganisms including bacteria, fungi and actinomycetes, which mediate nanoparticle formation through enzymatic and metabolite-driven pathways [9-11]. However, limitations such as the need for strict sterilized conditions, prolonged synthesis times and complex post-syn-

thesis processing have restricted their broader technological arrangement [12]. Animal-derived biomaterials such as egg albumin, gelatin and chitosan, offer alternative biological platforms but face challenges related to batch variability, stability and ethical considerations [13,14].

Among biological synthesis routes, the plant-mediated nanoparticle fabrication has emerged as a robust and scalable strategy within nanotechnology research [15]. Plant extracts are rich in diverse phytochemicals such as polyphenols, flavonoids, alkaloids, terpenoids and proteins that simultaneously act as reducing, capping and stabilizing agents, enabling controlled nanoparticle formation [16]. The simplicity of processing, reduced procedural complexity and ready availability of plant resources further enhance the suitability of this approach for large-scale nanoparticle production. Several medicinal plants such as *Azadirachta indica*, *Moringa oleifera*, *Aloe vera*, *Ocimum sanctum*, *Calotropis gigantea* and *Catharanthus roseus*, have been successfully employed in the green synthesis of zinc oxide (ZnO) nanoparticles, yielding materials with tailored physico-chemical properties and promising biological functions [17-22]. These studies collectively highlight plant-mediated synthesis as a viable nanotechnological platform for developing functional and biocompatible ZnO nanomaterials.

The genus *Kalanchoe*, belonging to the Crassulaceae family, comprises over 125 species of succulent plants, many of which are extensively used in traditional medicine across Asia, Africa and South America [23]. Several species such as *Kalanchoe pinnata*, *Kalanchoe crenata*, *Kalanchoe blossfeldiana* and *Kalanchoe laciniata* are known for their potent antimicrobial, antioxidant, anti-inflammatory, wound healing and anticancer properties. Phytochemical studies of these species have revealed the presence of alkaloids, flavonoids, phenolic acids, bufadienolides, triterpenes and steroids, which contribute to their bioactivity and also make them suitable candidates for metallic nanoparticle synthesis [24-27]. For instance, *K. pinnata* leaf extract has been utilized in the synthesis of silver (AgNPs), gold (AuNPs) and zinc oxide nanoparticles (ZnO NPs) [28,29]. These metallic nanoparticles have demonstrated enhanced antimicrobial activity on both Gram-positive and Gram-negative bacteria's, significant antioxidant potential in DPPH assays and cytotoxic effects against certain cancer cell lines. Similarly, *K. crenata*-derived AgNPs have shown efficacy in wound healing and anti-inflammatory models, underscoring the medicinal potential of this genus when combined with nanoscale materials [30,31].

Despite these promising results, most of the researches have been concentrated on a few well-known species, especially *K. pinnata* and *K. crenata*, while other phytochemically potent species like *Kalanchoe fedtschenkoi* remain underexplored. *K. fedtschenkoi*, an ornamental succulent native to Madagascar and widely cultivated in India, has shown preliminary evidence of antioxidant and antimicrobial properties [32,33]. However, its use in green nanotechnology, particularly for the synthesis of zinc oxide nanoparticles (ZnONPs), has not yet been systematically investigated.

Therefore, the present investigation emphasizes the plant mediated synthesis of ZnO nanoparticles using *K. fedtschenkoi* leaf extract (Kf-ZnNPs) to address existing gaps in green nanomaterial research. The synthesized nanoparticles were systematically characterized using UV-Visible spectroscopy, scanning electron microscopy (SEM), dynamic light scattering (DLS), zeta potential analysis, Fourier transform infrared spectroscopy (FTIR) and X-ray diffraction (XRD) to evaluate their optical, morphological, surface and crystalline properties. Furthermore, the biological performance of Kf-ZnNPs was assessed through *in vitro* assays to determine their antimicrobial efficacy against *Staphylococcus aureus*, *Escherichia coli* and *Candida albicans*, along with their antioxidant, antidiabetic, anti-inflammatory and anticancer activities.

EXPERIMENTAL

Plant extract: Fresh *Kalanchoe fedtschenkoi* leaves were collected from the Botanical Garden at S.M. Joshi College campus, Hadapsar, Pune, India. Under the authentication no. Bot/BGC-28/AUTH, the plant material was taxonomically verified and used. In brief, freshly harvested leaves (10 g) were thoroughly washed with distilled water to remove surface contaminants and then finely macerated using a mortar and pestle. The resulting paste was transferred to a beaker containing 100 mL of distilled water and heated at 70 ºC for 30 min under continuous stirring on a magnetic hot plate to enhance the extraction of phytochemicals. After cooling to room temperature, the extract was filtered through a 20 µm syringe filter to remove coarse particulates. The filtrate was subsequently centrifuged at 4000 rpm for 15 min to eliminate residual plant debris. The resulting clear supernatant was collected, sealed and stored at 4 ºC for subsequent use in the green synthesis of ZnO nanoparticles.

Synthesis of ZnO nanoparticles (Kf-ZnNPs): Phyto-capped ZnO nanoparticles (Kf-ZnNPs) were synthesized using an aqueous zinc acetate dihydrate solution (1.0 mM) as the precursor. To generate an alkaline medium favourable for nanoparticle formation, a 0.1 M NaOH solution was added dropwise under continuous magnetic stirring until the pH reached approximately 9. Subsequently, the previously prepared *K. fedtschenkoi* leaf extract was introduced into the reaction mixture in a 1:9 (v/v) ratio. The reaction was allowed to proceed under constant stirring at room temperature for 24 h. During the synthesis, the reaction mixture gradually changed from a milky appearance to a clear solution, with the simultaneous formation of a pale yellowish-white precipitate, indicating successful formation of ZnO nanoparticles. The resulting Kf-ZnNPs were collected by centrifugation at 14,000 rpm for 15 min and washed 2-3 times with distilled water to remove residual impurities and unreacted species. The obtained Kf-ZnNPs nanoparticles were then dried and stored for subsequent characterization and biological evaluation.

Characterization: The optical and structural characterization of *K. fedtschenkoi* mediated ZnO nanoparticles (Kf-ZnNPs) was carried out using multiple analytical techniques. UV-Vis spectroscopy was performed on a Shimadzu UV-1800 spectrophotometer in absorbance mode over 300-900 nm to compare the surface plasmon resonance of Kf-ZnNPs with the absorption profiles of the plant extract and 1 mM zinc acetate solution. FESEM (Nova NanoSEM NPEP303) operated at 15 kV under high vacuum was used to examine nanoparticle morphology and size. The hydrodynamic diameter and polydis-

persity index (PDI) were determined by dynamic light scattering (DLS) using a Brookhaven Instrument system, while the surface charge and colloidal stability were evaluated through zeta potential analysis employing phase analysis light scattering (PALS) at 25 ºC. Fourier transform infrared (FTIR) spectroscopy (Bruker) in the range of 4000-500 cm^{-1} was used to identify the functional groups responsible for nanoparticle reduction and stabilization. The crystalline structure and average crystallite size of Kf-ZnNPs were analyzed by X-ray diffraction (XRD) using Cu-*K*α radiation (λ = 1.5406 Å) over a 2θ range of 3-90º, with phase identification confirmed using JCPDS card no. 36-1451 and crystallite size estimated using the Debye-Scherrer's equation.

Biological activity assays

Antimicrobial activity: The antimicrobial activity of phyto-capped Kf-ZnNPs was assessed against Gram-positive *S. aureus* (ATCC 29213), Gram-negative *E. coli* (ATCC 25922) and the fungal strain *C. albicans* (ATCC 10231) using the agar-well diffusion method. For antibacterial evaluation, nutrient agar plates (HiMedia) were inoculated with 100 µL of bacterial suspension and uniformly spread, followed by aseptic punching of 6 mm diameter wells. Each well was loaded with 100 µL of Kf-ZnNPs solution (1 mg/mL in DMSO). Streptomycin (1 mg/mL) and DMSO served as positive and negative controls, respectively. For antifungal assessment, Sabouraud agar plates (HiMedia) were prepared and inoculated with 100 µL of fungal culture, after which wells of 3 mm radius were prepared and filled with 100 µL of Kf-ZnNPs solution (1 mg/mL in DMSO). Miconazole (1 mg/mL) and DMSO were used as positive and negative controls, respectively. All plates were incubated at 37 ºC for 24 h and antimicrobial activity was quantified by measuring the zones of inhibition in millimeters. Each experiment was performed in triplicate to ensure reproducibility.

Antioxidant activity: The antioxidant activity of Kf-ZnNPs was evaluated using the DPPH radical scavenging assay. Serial dilutions of the nanoparticles were prepared in methanol at concentrations ranging from 20 to 100 µg/mL. Each concentration was mixed with 1.5 mL of 0.1% methanolic DPPH solution and incubated in dark at room temperature for 30 min. The absorbance was measured at 510 nm using a colorimeter. All experiments were performed in triplicate and the mean absorbance values were used to calculate the percentage of radical scavenging activity using the standard DPPH formula. Ascorbic acid served as the positive control.

Anti-inflammatory activity: *In vitro* protein denaturation assay was performed to estimate the anti-inflammatory activity of Kf-ZnNPs [34]. Fresh egg albumin (0.4 mL), PBS (pH 6.4; 5.6 mL) and 100 µL of test sample at varying concentrations (20-100 µg/mL) were mixed to make 10 mL final volume. For 15 min incubation was performed at 37 ± 2 ºC, then for 5 min heating was done at 70 ºC and after subsequent cooling the absorbance was taken at 660 nm. For the positive control, diclofenac sodium was used and double distilled water as a blank was used. In triplicate all tests were performed. The percentage inhibition of protein denaturation was calculated using the standard formula:

$$\text{Inhibition (\%)} = \frac{C - T}{C} \times 100$$

where C = absorbance of control and T = absorbance of test sample.

Antidiabetic activity: The *in vitro* α-amylase inhibition assay was performed to assess the antidiabetic activity of biosynthesized Kf-ZnNPs using the Bernfeld method [35]. Different concentrations of the nanoparticles (20-100 µg/mL) were incubated with α-amylase enzyme and starch substrate in phosphate buffer (pH 6.9). After a second incubation, the reaction was halted using dinitrosalicylic acid (DNS) reagent and boiled. At 540 nm, the absorbance was recorded using a spectrophotometer. All the experimental conditions were performed in triplicates to ensure the reproducibility. The percentage inhibition of α-amylase was calculated by comparing the absorbance of control and treated samples. Acarbose was used as the standard reference drug.

Anticancer assay: The cytotoxic potential of biosynthesized phyto-capped Kf-ZnNPs was evaluated against human lung (A549) and breast (MCF-7) cancer cell lines using the standard MTT assay. Cells procured from the National Centre for Cell Science (NCCS), Pune, were cultured in DMEM supplemented with 10% fetal bovine serum and 1% penicillin-streptomycin and maintained at 37 ºC in a humidified incubator with 5% CO_2. At 70-80% confluence, cells were trypsinized (0.25% trypsin-EDTA), counted and seeded into 96-well plates at a density of 1×10^4 cells per well. After 24 h for cell attachment, the medium was replaced with fresh DMEM containing serial concentrations of Kf-ZnNPs (15.625-500 µg/mL). Docetaxel at corresponding concentrations was used as the positive control. Following 24 h of treatment, the medium was replaced with 100 µL of MTT solution (0.5 mg/mL) and incubated for 3 h to allow formazan formation. The resulting crystals were dissolved in 100 µL of DMSO and absorbance was measured at 570 nm using a microplate reader. Cell viability was expressed as a percentage relative to untreated controls and IC_{50} values were determined from dose-response curves using nonlinear regression. All experiments were performed in triplicate, and results are presented as mean ± standard deviation (SD).

Statistical analysis: All the biological activities were performed in triplicate set and the results expressed in mean ± standard deviation (SD). Statistical significance of differences between control, standard and test groups was evaluated using one-way analysis of variance (ANOVA) after that by Tukey's post-hoc test for multiple comparisons. A t-taste *p*-value if not greater that 0.05 ($p < 0.05$) then it is considered as statistically significant. Data analysis and graphical representations were performed using SPSS version 16.0 and Microsoft Excel 2016.

RESULTS AND DISCUSSION

The plant-mediated synthesis of ZnO nanoparticles (Kf-ZnNPs) using leaf extract from *K. fedtschenkoi* reflects an effective nanobiotechnological strategy for producing functional ZnO nanomaterials. Aqueous extraction under heating releases bioactive phytoconstituents such as flavonoids and polyphenols, which facilitate reduction and surface capping of nanoparticles [36]. The adjustment of reaction pH to approximately 9 enhances ZnO nucleation kinetics, consistent with

reported synthesis mechanisms [37]. Zinc acetate was chosen as the metal precursor owing to its high aqueous solubility and suitability for mild reaction environments. The formation of a white precipitate corresponds to ZnO NPs generation, as reported previously [38]. Post-synthesis purification ensured removal of residual organic and ionic species.

UV-Vis spectroscopy: The UV-visible absorption spectra (Fig. 1) compare the optical characteristics of (a) phyto-capped Kf-ZnNPs synthesized using *K. fedtschenkoi* leaf extract, (b) plant extract alone and (c) zinc acetate precursor solution. The spectrum of Kf-ZnNPs (Fig. 1a) exhibits a sharp and well-defined absorption peak at 349 nm, which is characteristic of the surface plasmon resonance (SPR) associated with ZnO NPs, confirming their successful formation and nanoscale nature [39]. A weak shoulder observed around 310 nm is attributed to the residual phytochemicals, such as flavonoids and phenolic compounds, that remain adsorbed on the nanoparticle surface and contribute to reduction and stabilization processes [40]. In contrast, the plant extract spectrum (Fig. 1b) shows a broad absorption band near 349 nm, arising from its inherent phyto-constituents, while the zinc acetate solution (Fig. 1c) displays negligible absorbance across the 300-800 nm range, indicating the absence of nanoparticle-related optical features. The absence of secondary peaks or extended absorption beyond 400 nm in the Kf-ZnNPs spectrum suggests a high degree of monodispersity, minimal aggregation and good optical purity. These spectral features are consistent with previously reported green-synthesized ZnO nanoparticles and further validate the effective role of *K. fedtschenkoi* extract in mediating the formation and stabilization of ZnO nanostructures [41,42].

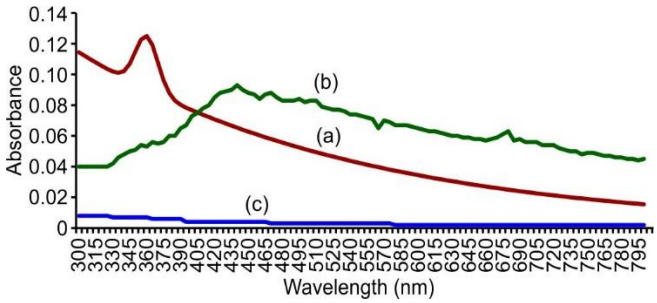

Fig. 1. UV-Vis absorption spectra of (a) Kf-ZnNPs, (b) *Kalanchoe fedtschenkoi* leaf extract and (c) zinc acetate

FESEM: FESEM analysis (Fig. 2) revealed that the bio-synthesized Kf-ZnNPs possess a predominantly quasi-spherical morphology with a narrow particle size distribution, confirming effective nanoscale control during synthesis. The particle sizes ranged from 13.49 to 24.28 nm, with an average diameter of 18.52 ± 3.12 nm, and most particles were clustered around ~18.9 nm, indicating the uniform growth behaviour. The fine granular surface texture and consistent nanoscale features suggest efficient reduction, capping and stabilization by phyto-chemicals present in the *K. fedtschenkoi* extract, in agreement with other plant-mediated ZnO nanoparticle studies [43-45]. Moderate agglomeration observed in the micrographs is likely attributable to phytochemical-mediated interparticle interactions and the drying process, as reported previously [46,47]. Similar quasi-spherical morphologies have been documented for ZnO NPs synthesized using *A. indica* and other medicinal

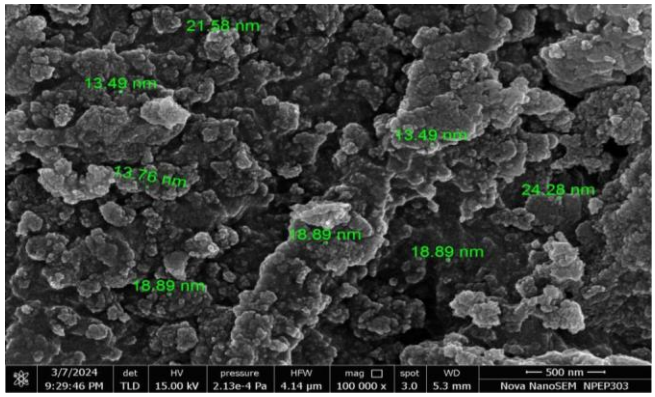

Fig. 2. FESEM image of Kf-ZnNPs

plant extracts [48]. Overall, the uniform morphology and reproducible size distribution validate the role of *K. fedtschenkoi* phytoconstituents in directing controlled green synthesis, a feature advantageous for biomedical applications due to enhanced surface reactivity and cellular interaction [20].

Dynamic light scattering (DLS): DLS analysis revealed that the hydrodynamic diameter of the Kf-ZnNPs ranged from 31.70 to 37.43 nm, with a mean particle size of 34.20 ± 2.93 nm (n = 3), as presented in Table-1 and Fig. 3. The polydispersity index (PDI) values varied between 0.001 and 0.306 (mean PDI: 0.205 ± 0.176), indicating a narrow size distribution and good colloidal stability. PDI values below 0.3 are indicative of moderate to high monodispersity, confirming that the nanoparticles were well dispersed in the aqueous medium with minimal aggregation. The intensity-based DLS profile displayed a single, sharp monomodal peak centered around 34.2 nm, reflecting uniform particle populations consistent with green-synthesized ZnO nanoparticles reported in earlier studies [49-52]. A baseline index of 0.0 across all measurements further confirmed instrumental stability and low background interference, supporting sample purity. The slightly larger hydrodynamic size observed by DLS compared to FESEM measurements can be attributed to the hydration layer and phytochemical capping on the nanoparticle surface. Overall, the DLS results are consistent with the FESEM findings and validate the reproducible synthesis of uniformly sized, colloidally stable Kf-ZnNPs mediated by plant phytoconstituents.

TABLE-1
DYNAMIC LIGHT SCATTERING (DLS) ANALYSIS OF BIOSYNTHESIZED Kf-ZnNPs

Sample ID	Effective diameter (nm)	Polydispersity index	Baseline index
Zn-1	37.43	0.306	0.0
Zn-2	31.70	0.001	0.0
Zn-3	33.48	0.306	0.0
Mean	34.20	0.205	0.0
Std. error	1.70	0.102	0.0
Std. deviation	2.93	0.176	–

Zeta potential: The zeta potential measurements of Kf-ZnNPs revealed moderately negative surface charges ranging from -8.68 to -14.96 mV, with an average value of -11.66 ± 3.15 mV (n = 3), as illustrated in Table-2 and Fig. 4. These values indicate sufficient electrostatic repulsion among particles

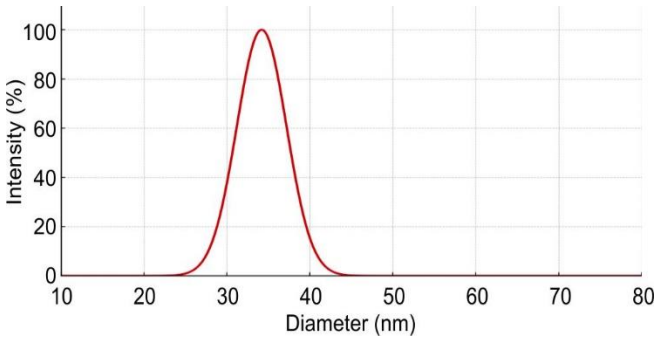

Fig. 3. Intensity-based DLS size distribution of Kf-ZnNPs

TABLE-2
ZETA POTENTIAL MEASUREMENTS
OF BIOSYNTHESIZED Kf-ZnNPs

Sample ID	Zeta potential (mV)	Electrophoretic mobility (μs/V cm)	RMS residual
Zn-1	–8.68	–0.68	3.19×10^{-2}
Zn-2	–11.35	–0.89	1.55×10^{-2}
Zn-3	–14.96	–1.17	2.49×10^{-2}
Mean	–11.66	–0.91	2.41×10^{-2}
Std. error	1.82	0.14	4.75×10^{-3}
Std. deviation	3.15	0.25	8.22×10^{-3}

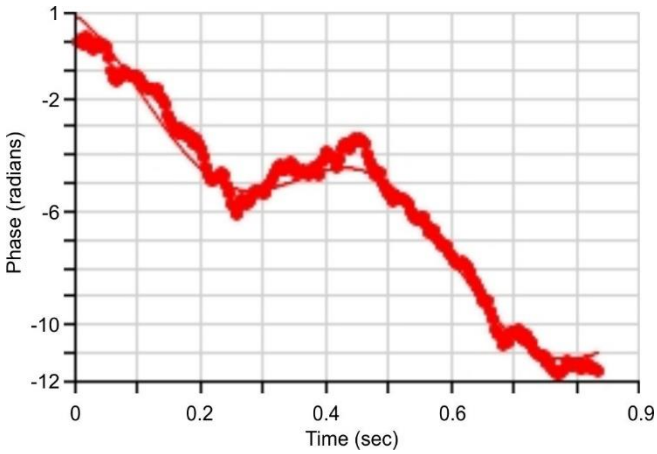

Fig. 4. PALS (phase analysis light scattering) graph showing the phase shift curve of biosynthesized Kf-ZnNPs, used to calculate zeta potential through time-resolved signal interpretation

to support colloidal stability in aqueous suspension, despite being below the conventional ±30 mV threshold typically associated with highly stable dispersions. The nanoparticles remained well dispersed throughout characterization, consistent with DLS and FESEM observations. Electrophoretic mobility values ranged from -0.68 to -1.17 μs/V cm (mean: -0.91 ± 0.25 μs/V cm), confirming the presence of negatively charged and mobile nanoparticle surfaces. Low RMS residual values (mean: 2.41×10^{-2}) further indicate reliable measurement fitting with minimal background interference. The observed surface charge is attributed to phytochemical constituents from the *K. fedtschenkoi* extract, which act as capping agents and impart electrostatic stabilization. Comparable zeta potential values have been reported for ZnO NPs synthesized *via* other plant-mediated routes, supporting the reproducibility and stability of the green synthesis approach [53-57].

FTIR studies: The FTIR spectrum of the biosynthesized Kf-ZnNPs (Fig. 5) displayed multiple characteristic absorption bands, confirming the involvement of plant-derived phytochemicals in nanoparticle formation and stabilization. A broad and intense band at 3396.08 cm^{-1} is attributed to O–H stretching vibrations of phenolic or alcoholic groups, indicating the presence of polyphenolic compounds from the *K. fedtschenkoi* extract [58]. The weak absorption observed near 2923.82 cm^{-1} corresponds to C–H stretching of aliphatic $–CH_2$ groups, commonly associated with plant-based organic constituents. Prominent peaks in the fingerprint region at 1572.53, 1442.95 and 1365.34 cm^{-1} are assigned to N–H bending of amines or amides, C=C stretching of aromatic rings and C–N stretching vibrations of proteins or alkaloids, respectively, suggesting the role of nitrogen-containing biomolecules as capping and stabilizing agents [59,60]. Additional sharp bands at 1212.81 and 1056.26 cm^{-1} correspond to C–O stretching vibrations of alcohols, esters or ethers, further supporting the presence of organic moieties on the nanoparticle surface. Notably, absorption bands below 1000 cm^{-1}, including peaks at 826.89, 667.38 and 558.60 cm^{-1}, are characteristic of Zn–O stretching vibrations, confirming the formation of the ZnO nanoparticle framework [53]. Collectively, these FTIR findings demonstrate that biomolecules present in the *K. fedtschenkoi* extract actively participate in the reduction of Zn^{2+} ions and provide effective surface capping and stabilization to the synthesized Kf-ZnNPs.

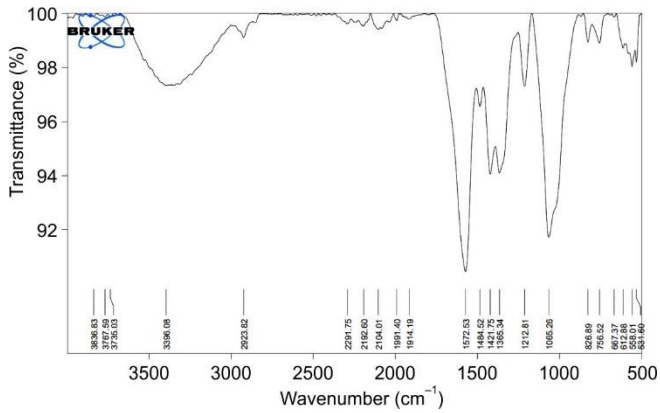

Fig. 5. FTIR spectrum of Kf-ZnNPs

XRD studies: The X-ray diffraction (XRD) pattern of the biosynthesized Kf-ZnNPs exhibited well-defined and intense Bragg reflections at 2θ values of 31.78º, 34.45º, 36.27º, 47.53º and 56.60º, corresponding to the (100), (002), (101), (102), and (110) crystallographic planes, respectively (Fig. 6). These diffraction peaks are in excellent agreement with the standard data for hexagonal wurtzite ZnO (JCPDS card No. 36-1451), confirming the formation of a pure crystalline phase without detectable secondary or impurity phases [58]. The calculated interplanar spacings (*d*-values) ranged from 1.624 to 2.814 Å, consistent with the ZnO lattice parameters. Crystallite sizes estimated using the Debye-Scherrer's equation from the most intense reflections were in the nanoscale range, with values spanning approximately 17.7 to 26.4 nm and an average crystallite size of 21.78 ± 3.42 nm (Table-3). The narrow FWHM values (0.0055-0.0081 radian) and high peak inten-

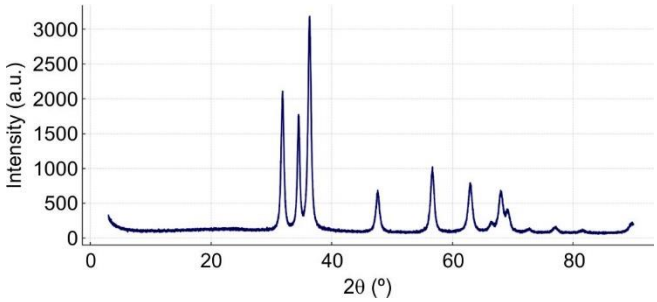

Fig. 6. XRD pattern of biosynthesized Kf-ZnNPs

TABLE-3
MAJOR XRD PEAKS OF Kf-ZnNPs
WITH INTERPLANAR SPACING, FWHM,
CRYSTALLITE SIZE AND INDEXED PLANES

2θ (°)	d-spacing (Å)	FWHM (β, rad)	Crystallite size (nm)	Indexed plane (*hkl*)
31.78	2.814	0.0055	26.4	(100)
34.45	2.603	0.0060	24.0	(002)
36.27	2.474	0.0070	22.3	(101)
47.53	1.913	0.0081	17.7	(102)
56.60	1.624	0.0078	18.5	(110)

sities indicate excellent crystallinity with the minimal lattice strain or structural defects. These results confirm the successful green synthesis of phase-pure, highly crystalline ZnO NPs using *K. fedtschenkoi* extract and are consistent with the particle morphology observed by FESEM and the size distribution obtained from DLS analysis.

Biological activities

Antimicrobial activity: The antimicrobial efficacy of the biosynthesized Kf-ZnNPs (1 mg/mL) was evaluated using the agar well diffusion method against *S. aureus*, *E. coli* and *C. albicans*, and the results are shown in Table-4. Kf-ZnNPs exhibited pronounced antibacterial activity, producing inhibition zones of 25.00 ± 1.00 mm against *S. aureus* and 22.00 ± 1.00 mm against *E. coli*, indicating strong and reproducible antibacterial potential. In comparison, the standard antibiotic streptomycin (1 mg/mL) produced slightly larger inhibition zones of 31.00 ± 1.00 mm and 30.00 ± 1.00 mm, respectively, while the negative control (DMSO) showed no inhibitory effect, confirming assay specificity [61,62]. Statistical analysis using a t-test demonstrated significant differences ($p \leq 0.05$) between Kf-ZnNPs and the control, with *S. aureus* displaying greater susceptibility than *E. coli*. The observed antibacterial activity is consistent with previously reported mechanisms for ZnO NPs, including reactive oxygen species generation, membrane disruption, and metal ion release, which are enhanced by the nanoscale size and high surface area of the particles [63,64]. In antifungal assays, Kf-ZnNPs showed substantial inhibitory activity against *C. albicans*, producing a clear zone of inhibition measuring 23.00 ± 1.00 mm, closely comparable to the standard antifungal drug miconazole (26.00 ± 1.00 mm). The absence of inhibition in the DMSO control confirmed that the antifungal effect was solely attributable to the nanoparticles. Statistical evaluation ($p \leq 0.05$) indicated significant inhibition by both Kf-ZnNPs and miconazole relative to the control. Comparable antifungal activities have been reported for ZnO NPs synthesized using plant extracts such as *Lavandula angustifolia* and *Salvia officinalis*, suggesting that plant-derived metabolites play a key role in enhancing antifungal efficacy [65-67]. The antifungal mechanism is likely associated with membrane damage and oxidative stress in fungal cells, as proposed in earlier nanoparticle-based studies [68,69]. Overall, these findings demonstrate the broad-spectrum antibacterial and antifungal potential of Kf-ZnNPs synthesized using *K. fedtschenkoi*, supporting their promise as effective green nanomaterials.

Antioxidant activity: The antioxidant potential of the biosynthesized Kf-ZnNPs was evaluated using the DPPH radical scavenging assay and the results are illustrated in Fig. 7. Kf-ZnNPs exhibited a clear concentration-dependent increase in percentage inhibition across the tested range of 20-100 µg/mL, following a trend similar to that of the standard antioxidant ascorbic acid. Notably, at 40 µg/mL, the scavenging activity of Kf-ZnNPs was statistically comparable to ascorbic acid, demonstrating appreciable antioxidant efficacy even at moderate concentrations. At the highest concentration (100 µg/mL), Kf-ZnNPs achieved a maximum inhibition of 55.95 ± 1.56%, whereas ascorbic acid showed a higher inhibition of 82.86 ± 0.95%. The IC_{50} value of Kf-ZnNPs was calculated to be 92 µg/mL, confirming effective free-radical scavenging capacity. Statistical analysis ($p \leq 0.05$) indicated significant differences among concentrations and between treatments. Although the antioxidant activity of Kf-ZnNPs was lower

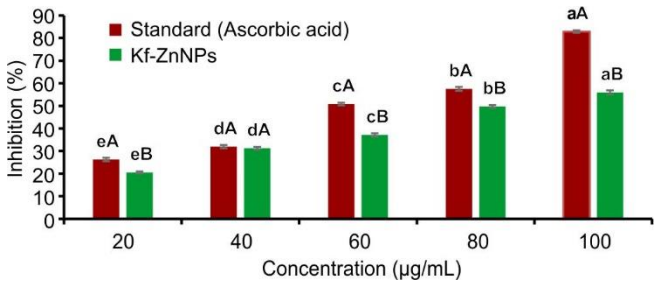

Fig. 7. DPPH radical scavenging activity of Kf-ZnNPs and ascorbic acid at different concentrations. Different lowercase letters indicate significant differences within groups; uppercase letters show differences between groups ($p \leq 0.05$)

TABLE-4
ANTIMICROBIAL ACTIVITY OF Kf-ZnNPs

Treatment	*Staphylococcus aureus*	*Escherichia coli*	*Candida albicans*
Control (DMSO)	0.00 ± 0.00	0.00 ± 0.00^{c}	0.00 ± 0.00^{c}
Standard (streptomycin)	31.00 ± 1.00^{a}	30.00 ± 1.00^{a}	Not applicable
Standard (miconazole)	Not applicable	Not applicable	26.00 ± 1.00^{a}
Kf-ZnNP (1 mg/mL)	25.00 ± 1.00^{b}	22.00 ± 1.00^{b}	23.00 ± 1.00^{b}

The zone of inhibition (mm) are expressed as mean ± SD (n = 3). The small letter denotes the significant antimicrobial activity at $p < 0.05$.

than that of the standard, it remains biologically meaningful and is consistent with previous reports on green-synthesized ZnO NPs derived from *Moringa oleifera* and *Azadirachta indica* [70,71]. The observed activity is largely attributed to the surface-bound phytochemicals retained from *K. fedtschenkoi* extract, which act as electron donors and enhance redox behaviour, in agreement with earlier studies on the polyphenol-stabilized nanoparticles [72-74].

Anti-inflammatory activity: The anti-inflammatory potential of the biosynthesized Kf-ZnNPs was evaluated using the heat-induced protein denaturation inhibition assay, and the results are shown in Fig. 8. Biosynthesized Kf-ZnNPs exhibited a clear concentration-dependent increase in inhibitory activity across the tested range of 20-100 µg/mL. At the highest concentration (100 µg/mL), the nanoparticles showed substantial inhibition of protein denaturation (≈62%), whereas the standard anti-inflammatory drug diclofenac sodium produced a higher inhibition (≈87%), confirming the validity of the assay. The IC_{50} value of Kf-ZnNPs (70.98 µg/mL) was comparable to that of diclofenac sodium (68.70 µg/mL), indicating similar efficacy in suppressing protein denaturation. Statistical analysis ($p \leq 0.05$) demonstrated significant differences between concentrations and treatments. Comparable protein stabilization effects have been reported for ZnO NPs synthesized using plant extracts such as *Camellia sinensis* and *Aframomum citratum* [75-77]. The observed anti-inflammatory activity is attributed to phytochemical residues on the nanoparticle surface, which may protect proteins from structural deformation under thermal stress [78]. Consistent with earlier findings by Ragavan [79], these results suggest that phyto-capped ZnO NPs represent promising, biocompatible alternatives for inflammation management [79].

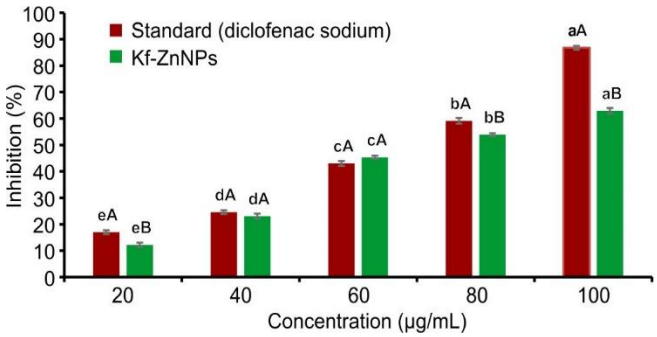

Fig. 8. Comparative anti-inflammatory activity of Kf-ZnNPs and diclofenac sodium (standard) in protein denaturation inhibition assay (20-100 µg/mL). Data presented as mean ± SD (n = 3). Lowercase letters indicate significant differences between concentrations and uppercase letters show differences between treatments ($p \leq 0.05$)

Antidiabetic activity: The antidiabetic potential of the biosynthesized Kf-ZnNPs was evaluated using the α-amylase inhibition assay and the results are presented in Fig. 9. Kf-ZnNPs exhibited a clear concentration-dependent inhibitory effect, with enzyme inhibition increasing progressively and reaching 52.87 ± 1.73% at 100 µg/mL. In comparison, standard antidiabetic drug acarbose showed a higher inhibition of 84.48% at the same concentration, confirming the reliability of the assay. The IC_{50} value of Kf-ZnNPs was calculated to be 97.13 µg/mL, indicating moderate yet significant α-amylase

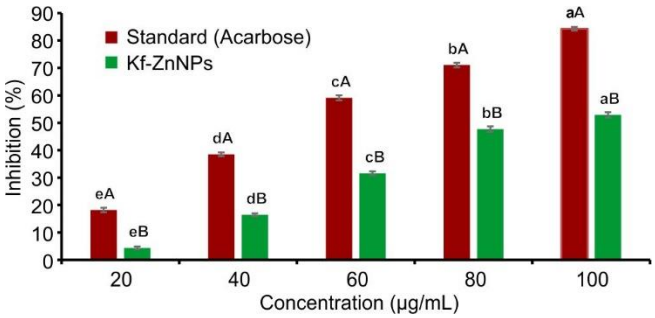

Fig. 9. α-Amylase inhibition activity of Kf-ZnNPs and standard acarbose at various concentrations, showing dose-dependent antidiabetic potential

inhibitory activity, whereas acarbose displayed a lower IC_{50} value (≈68.13 µg/mL), reflecting its stronger potency. The statistical analysis revealed significant differences ($p \leq 0.05$) among concentrations for both Kf-ZnNPs and the standard, particularly at higher doses. Notably, Kf-ZnNPs demonstrated consistent and meaningful inhibition in the 60-80 µg/mL range, where their activity closely approached that of acarbose. The observed enzyme inhibition is likely associated with interactions between the nanoparticles and the α-amylase active site, facilitated by their nanoscale dimensions and surface-bound phytochemicals [80]. Similar α-amylase inhibitory effects have been reported for ZnO NPs synthesized using *Helichrysum cymosum* and *Acacia nilotica* extracts, supporting the role of plant-derived capping agents in modulating carbohydrate metabolism [81-83]. Overall, these findings substantiate the antidiabetic potential of Kf-ZnNPs and highlight their promise as a plant-mediated, eco-friendly therapeutic alternative.

Anticancer assay: The cytotoxic activity of biosynthesized Kf-ZnNPs was evaluated against human lung (A549) and breast (MCF-7) cancer cell lines using the MTT assay following 24 h exposure. In A549 cells, Kf-ZnNPs induced a pronounced dose-dependent reduction in cell viability (Fig. 10), with viability decreasing to 6.76% at 500 µg/mL. The calculated IC_{50} value was 20.15 µg/mL, which is comparable to that of the standard anticancer drug docetaxel (15 µg/mL), indicating strong antiproliferative activity. Statistical analysis confirmed significant differences ($p \leq 0.05$) across concentrations and between treatments.

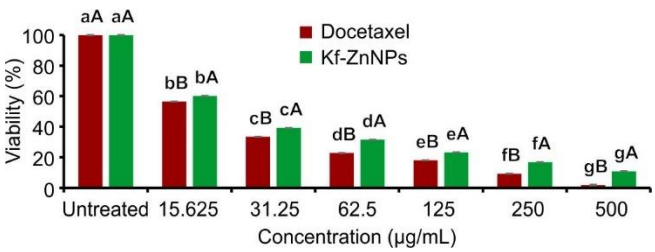

Fig. 10. Cell viability of A549 cells after treatment with Kf-ZnNPs and docetaxel. Lowercase and uppercase letters indicate significant differences within and between treatment groups, respectively ($p \leq 0.05$)

Morphological examination revealed that untreated A549 cells retained their characteristic elongated morphology and intact monolayer, whereas Kf-ZnNP-treated cells exhibited classical apoptotic features such as cell shrinkage, rounding,

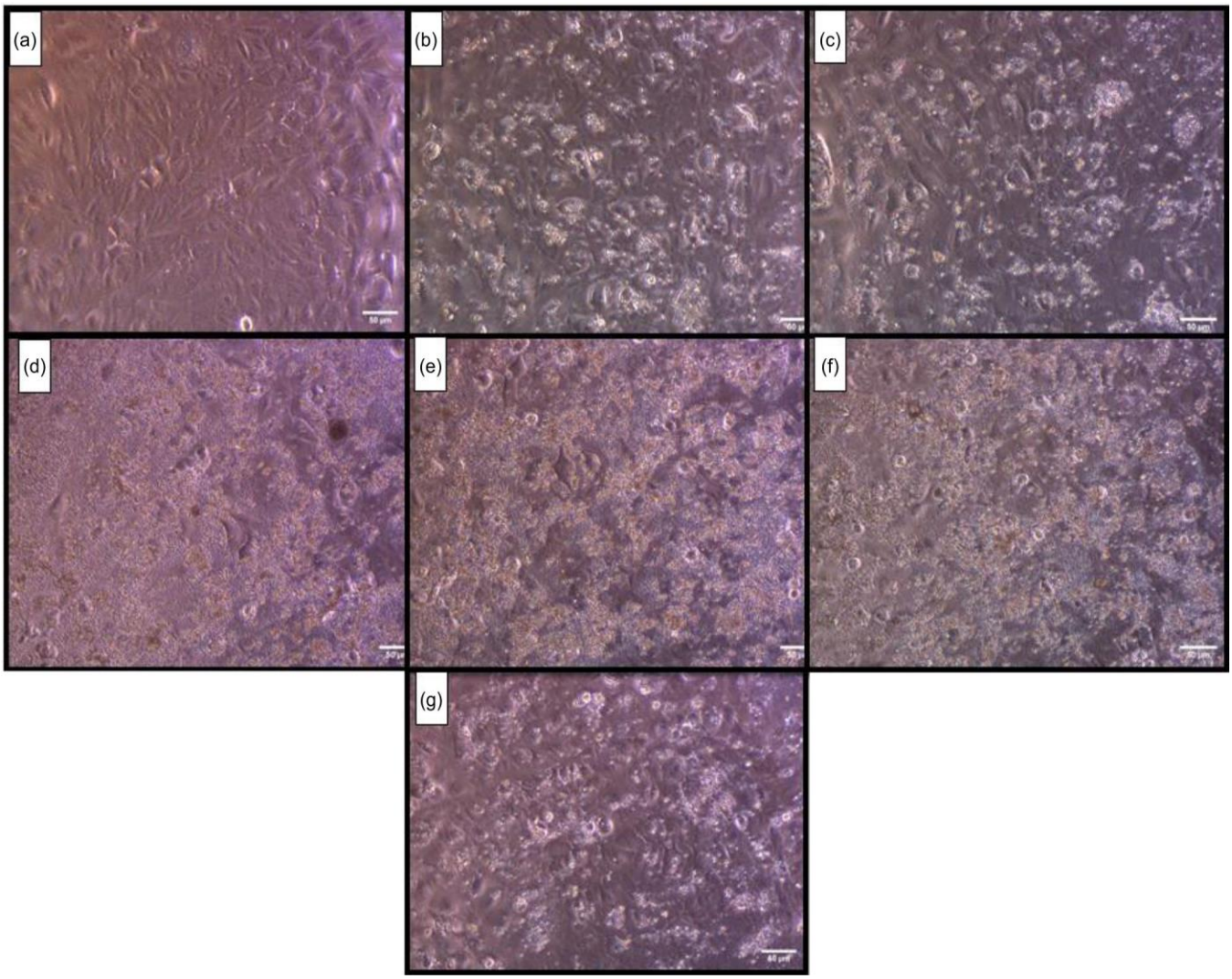

Fig. 11. Microscopic morphology of A549 cells post 24 h Kf-ZnNPs treatment: (a) Control, (b) 15.625, (c) 31.25, (d) 62.5, (e) 125, (f) 250, (g) 500 µg/mL

membrane blebbing and detachment, with severity increasing at higher concentrations (Fig. 11). Similarly, MCF-7 cells showed marked concentration-dependent cytotoxicity, with cell viability reduced to 5.71% at 500 µg/mL and an IC_{50} value of 15 µg/mL, compared to 9 µg/mL for docetaxel, reflecting greater sensitivity of this cell line (Fig. 12). Corresponding morphological changes including membrane disruption, vacuolation, rounding, and loss of adherence, were evident in treated MCF-7 cells (Fig. 13), supporting the viability data. These findings demonstrate that Kf-ZnNPs exert significant anticancer effects against both lung and breast cancer cells, consistent with earlier reports on green-synthesized ZnO NPs derived from plant sources such as *Terminalia arjuna* and *Mangifera indica* [84,85]. The observed cytotoxicity is likely mediated through mechanisms involving oxidative stress generation, mitochondrial dysfunction and apoptosis induction, as supported by prior studies on ZnO NPs-based anticancer systems [86-88]. Based on these results, the potential of phytochemically rich *K. fedtschenkoi* mediated ZnO NPs is highlighted as promising plant-based nanotherapeutic agents for cancer treatment.

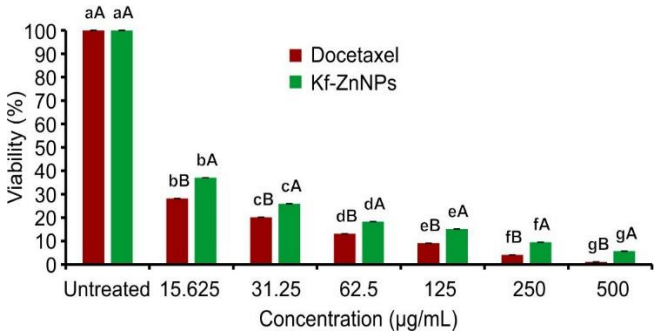

Fig. 12. Viability of MCF-7 cells after treatment with Kf-ZnNPs and docetaxel. Values are mean ± SD (n = 3). Lowercase and uppercase letters indicate significant intra- and inter-group differences ($p \leq 0.05$)

Conclusion

The present study reports the ecofriendly synthesis of phyto-capped zinc oxide nanoparticles (Kf-ZnNPs) using the aqueous leaf extract of *Kalanchoe fedtschenkoi*, a plant species underexplored for nanomaterial fabrication. The comprehensive characterization confirmed monodispersity, quasi-spherical

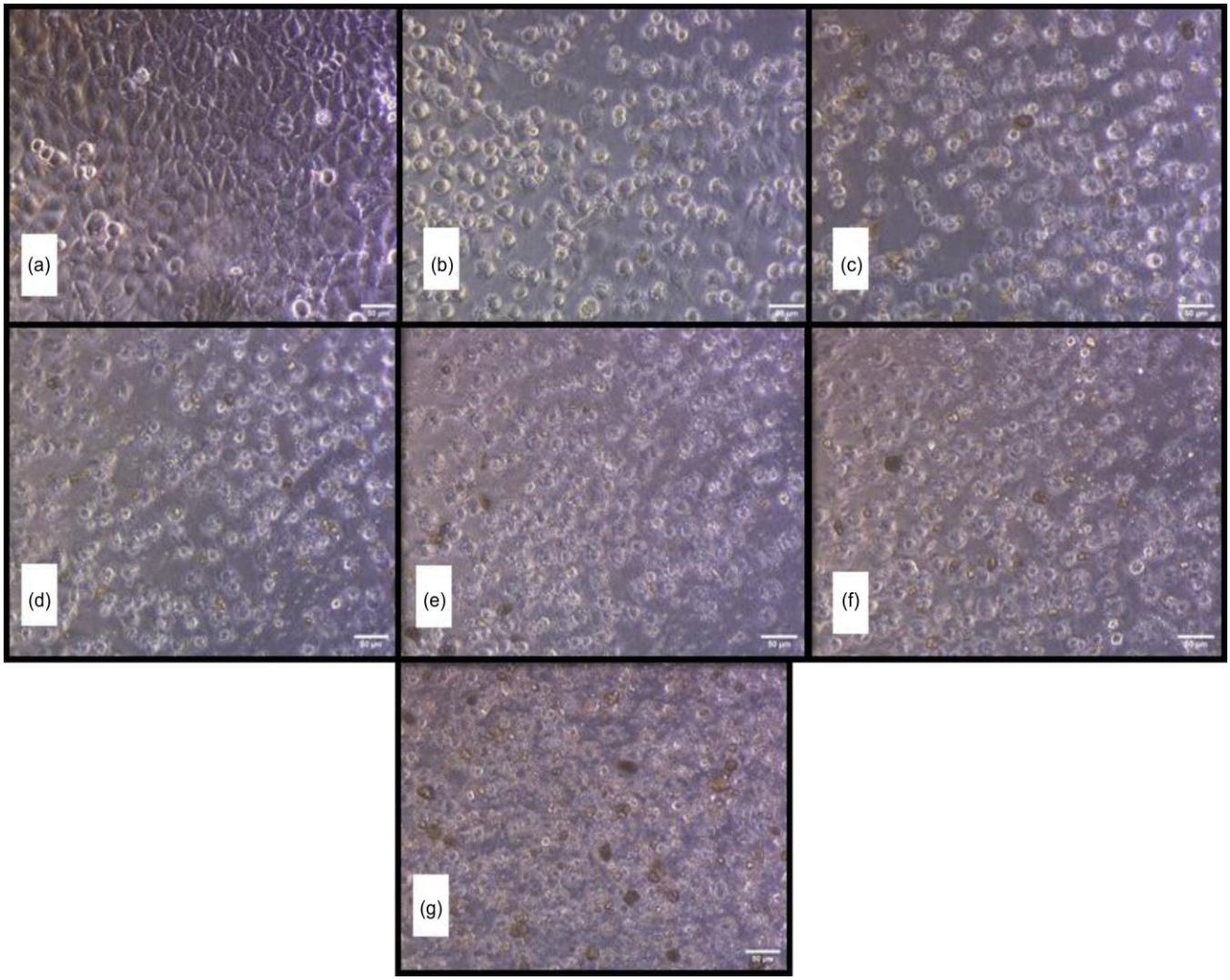

Fig. 13. Morphological changes in MCF-7 cells post 24 h Kf-ZnNPs treatments: (a) Control, (b) 15.625, (c) 31.25, (d) 62.5, (e) 125, (f) 250, (g) 500 µg/mL

morphology, moderate zeta potential and crystalline wurtzite structure as validated by UV-Vis, SEM, DLS, FTIR and XRD analyses. These structural and surface features contributed to their multifunctional bioactivities including pronounced antibacterial, antioxidant, anti-inflammatory, antidiabetic, antifungal and anticancer effects. Cytotoxic assays revealed potent and selective inhibition of A549 and MCF-7 cancer cell lines, underscoring their therapeutic potential. The enhanced performance is attributed to the synergistic influence of nanoscale dimensions and phytochemical surface functionalization. Overall, the findings establish *K. fedtschenkoi* as a sustainable plant resource for green nanotechnology, while highlighting the biomedical and environmental promise of Kf-ZnNPs. Future work should focus on *in vivo* validation and mechanistic studies to advance towards clinical and industrial applications.

ACKNOWLEDGEMENTS

The authors are grateful to the Prof. Ramkrishna More College, Akurdi, Pune and S.M. Joshi College, Hadapsar, Pune, for providing the laboratory as well as research facilities.

CONFLICT OF INTEREST

The authors declare that there is no conflict of interests regarding the publication of this article.

DECLARATION OF AI-ASSISTED TECHNOLOGIES

The authors declare that no AI tools were used in the preparation or writing of this research/review article.

REFERENCES

1. S. Iravani, *Green Chem.*, **13**, 2638 (2011); https://doi.org/10.1039/c1gc15386b
2. L.V. Srinivasan and S.S. Rana, *Discov. Appl. Sci.*, **6**, 371 (2024); https://doi.org/10.1007/s42452-024-06040-8
3. P. Szczyglewska, A. Feliczak-Guzik and I. Nowak, *Molecules*, **28**, 4932 (2023); https://doi.org/10.3390/molecules28134932
4. K. Hachem, M.J. Ansari, R.O. Saleh, H.H. Kzar, M.E. Al-Gazally, U.S. Altimari, S.A. Hussein, H.T. Mohammed, A.T. Hammid and E. Kianfar, *BioNanoScience*, **12**, 1032 (2022); https://doi.org/10.1007/s12668-022-00996-w

5. P. Champaneria, H. Sonawane, D. Shelke, M. Chambhare, K. More, S. Math and B. Zaware, *Plant Nano Biol.*, **9**, 100092 (2024); https://doi.org/10.1016/j.plana.2024.100092
6. M.S. Samuel, M. Ravikumar, A. John J, E. Selvarajan, H. Patel, P.S. Chander, J. Soundarya, S. Vuppala, R. Balaji and N. Chandrasekar, *Catalysts*, **12**, 459 (2022); https://doi.org/10.3390/catal12050459
7. J. Singh, T. Dutta, K.H. Kim, M. Rawat, P. Samddar and P. Kumar, *J. Nanobiotechnology*, **16**, 84 (2018); https://doi.org/10.1186/s12951-018-0408-4
8. I. Hussain, N.B. Singh, A. Singh, H. Singh and S.C. Singh, *Biotechnol. Lett.*, **38**, 545 (2016); https://doi.org/10.1007/s10529-015-2026-7
9. D.B. Shelke, N.F. Islam, M.R. Chambhare, H.B. Sonawane, R. Patowary, R. Prasad and H. Sarma, *Biocatal. Agric. Biotechnol.*, **52**, 102805 (2023); https://doi.org/10.1016/j.bcab.2023.102805
10. H. Sonawane, D. Shelke, M. Chambhare, N. Dixit, S. Math, S. Sen, S.N. Borah, N.F. Islam, S.J. Joshi, B. Yousaf, J. Rinklebe and H. Sarma, *Environ. Res.*, **212**, 113543 (2022); https://doi.org/10.1016/j.envres.2022.113543
11. N.I. Hulkoti and T.C. Taranath, *Colloids Surf. B Biointerfaces*, **121**, 474 (2014); https://doi.org/10.1016/j.colsurfb.2014.05.027
12. G. Grasso, D. Zane and R. Dragone, *Nanomaterials*, **10**, 11 (2019); https://doi.org/10.3390/nano10010011
13. M. Velhal, M. Dave, E. Sun, S. Holla and H. Liang, *Mater. Today Sustain.*, **27**, 100885 (2024); https://doi.org/10.1016/j.mtsust.2024.100885
14. R. .J. Babu, M. Annaji, A. Alsaqr and R.D. Arnold, *Polymeric Nanoparticles as a Promising Tool for Anti-cancer Therapeutics*, 319–341 (2019); https://doi.org/10.1016/B978-0-12-816963-6.00015-7
15. M.A. Dheyab, N. Oladzadabbasabadi, A.A. Aziz, P.M. Khaniabadi, M.T.S. Al-ouqaili, M.S. Jameel, F.S. Braim, B. Mehrdel and M. Ghasemlou, *J. Environ. Chem. Eng.*, **12**, 112345 (2024); https://doi.org/10.1016/j.jece.2024.112345
16. Z. Villagrán, L.M. Anaya-Esparza, C.A. Velázquez-Carriles, J.M. Silva-Jara, J.M. Ruvalcaba-Gómez, E.F. Aurora-Vigo, E. Rodríguez-Lafitte, N. Rodríguez-Barajas, I. Balderas-León and F. Martínez-Esquivias, *Resources*, 13, 70 (2024); https://doi.org/10.3390/resources13060070
17. N. Kumar, J. Jyoti, N. Aggarwal, A. Kaur, P. Patial, K. Kaur, S. Tripathi, S. Singh and V. Raja, *Biomass Convers. Biorefin.*, **14**, 30601 (2024); https://doi.org/10.1007/s13399-024-05419-2
18. B.S. Shashikala, K.R. Ashwini, D.R. Lavanya, Y. Jessica, P. Ushasri, D.V. Sunitha, G. Shobha, P.P.P. Dsouza and K.C.B. Naidu, *Inorg. Chem. Commun.*, **170**, 113355 (2024); https://doi.org/10.1016/j.inoche.2024.113355
19. M. Ashokkumar, K. Palanisamy, A. Ganesh Kumar, C. Muthusamy and K.J. Senthil Kumar, *Artif. Cells Nanomed. Biotechnol.*, **52**, 438 (2024); https://doi.org/10.1080/21691401.2024.2399938
20. C. Wu, T. Zhang, B. Ji, Y. Chou and X. Du, *Cellulose*, **31**, 4849 (2024); https://doi.org/10.1007/s10570-024-05914-9
21. J. C, R. Periakaruppan, V. Romanovski, K.S. Vijai Selvaraj and N. Al-Dayan, *Eng.*, **5**, 1399 (2024); https://doi.org/10.3390/eng5030073
22. A.B. Davlatov, A.H. Hameed, K. Feddi, P.J. Baymatov, B.T. Abdulazizov, A.A. Abdukarimov, A.G. Al-Shatravi, A.H. Al-Khursan, L.M. Pérez, D. Laroze and E. Feddi, *Appl. Phys., A Mater. Sci. Process.*, **131**, 1 (2025); https://doi.org/10.1007/s00339-024-08057-7
23. E. Assis de Andrade, I. Machinski, A.C. Terso Ventura, S.A. Barr, A.V. Pereira, F.L. Beltrame, W.K. Strangman and R.T. Williamson, *Molecules*, **28**, 5574 (2023); https://doi.org/10.3390/molecules28145574
24. L.B.S. Nascimento, L.M. Casanova and S.S. Costa, *Life*, **13**, 646 (2023); https://doi.org/10.3390/life13030646
25. T. Dimo, A. Fotio, T. Nguelefack, E. Asongalem and P. Kamtchouing, *Indian J. Pharmacol.*, **38**, 115 (2006); https://doi.org/10.4103/0253-7613.24617
26. J. Stefanowicz-Hajduk, A. Nowak, A. Hering, Ł. Kucharski, P. Graczyk, M. Kowalczyk, T. Sulikowski and A. Muzykiewicz-Szymańska, *Molecules*, **29**, 5548 (2024); https://doi.org/10.3390/molecules29235548
27. E.E.A. Osman, A.S. Mohamed, A. Elkhateeb, A. Gobouri, M.M. Abdel-Aziz and E.S.S. Abdel-Hameed, *Eur. J. Integr. Med.*, **49**, 102085 (2022); https://doi.org/10.1016/j.eujim.2021.102085
28. S.J. Nadaf, N.R. Jadhav, H.S. Naikwadi, P.L. Savekar, I.D. Sapkal, M.M. Kambli and I.A. Desai, *OpenNano*, **8**, 100076 (2022); https://doi.org/10.1016/j.onano.2022.100076
29. R. Jagdish and K. Nehra, *Heliyon*, **8**, e11080 (2022); https://doi.org/10.1016/j.heliyon.2022.e11080
30. S. Rajeshkumar and T. Lakshmi, *Int. J. Dent. Oral Sci.*, **8**, 2981 (2021).
31. M. Guleriya, S. Sinha, K. Pant, P. Gururani, N. Singh, J.M. Rawat, N.C. Joshi, S.G. Henao, D. Mitra, R. Sami, H.F. Al-Harthi, R.H. Kadi, N.I. Aljuraide and R.I. Bedaiwi, *Pol. J. Environ. Stud.*, **34**, 6163 (2025); https://doi.org/10.15244/pjoes/191975
32. J.M. Casanova, L.B. dos Santos Nascimento, L.M. Casanova, S.D. Castricini, J.E. de Souza, R.M.K. Yien, S.S. Costa and E.S. Tavares, *J. Appl. Bot. Food Qual.*, **95**, 154 (2022); https://doi.org/10.5073/JABFQ.2022.095.020
33. N. Richwagen, J.T. Lyles, B.L.F. Dale and C.L. Quave, *Front. Pharmacol.*, **10**, 67 (2019); https://doi.org/10.3389/fphar.2019.00067
34. B.H. Shnawa, P.J. Jalil, R.M. Mhammedsharif, B.A. Faqe, M.H. Ahmed, H.N. Ibrahim and M.H. Ahmed, *Part. Part. Syst. Charact.*, **41**, 2400005 (2024); https://doi.org/10.1002/ppsc.202400005
35. S.R. Abhinaya and R. Padmini, *Asian J. Pharm. Clin. Res.*, **12**, 245 (2019); https://doi.org/10.22159/ajpcr.2019.v12i1.28682
36. F. Zhou, T. Peterson, Z. Fan and S. Wang, *Nutrients*, **15**, 3881 (2023); https://doi.org/10.3390/nu15183881
37. R. Wahab, S.G. Ansari, Y.S. Kim, M. Song and H.S. Shin, *Appl. Surf. Sci.*, **255**, 4891 (2009); https://doi.org/10.1016/j.apsusc.2008.12.037
38. S. Kaenphakdee, P. Putthithanas, S. Yodyingyong, J. Leelawattanachai, W. Triampo, N. Sanpo, J. Jitputti and D. Triampo, *Materials*, **15**, 570 (2022); https://doi.org/10.3390/ma15020570
39. A. Aldalbahi, S. Alterary, R.A.A. Almoghim, M.A. Awad, N.S. Aldosari, S.F. Alghannam, A.N. Alabdan, S. Alharbi, B.A.M. Alateeq, A.A. Al Mohsen, M.A. Alkathiri and R. A. Alrashed, *Molecules*, **25**, 4198 (2020); https://doi.org/10.3390/molecules25184198
40. M.M. Caldwell, R. Robberecht and S.D. Flint, *Physiol. Plant.*, **58**, 445 (1983); https://doi.org/10.1111/j.1399-3054.1983.tb04206.x
41. A. Dey and S. Somaiah, *Microsc. Res. Technol.*, **85**, 2835 (2022); https://doi.org/10.1002/jemt.24132
42. M. Naseer, U. Aslam, B. Khalid and B. Chen, *Sci. Rep.*, **10**, 9055 (2020); https://doi.org/10.1038/s41598-020-65949-3
43. R.Z. Obaid, R. Abu-Huwaij and R. Hamed, *Jordan J. Pharm. Sci.*, **16**, 486 (2023); https://doi.org/10.35516/jjps.v16i2.1545
44. H. Agarwal, S.V. Kumar and S. Rajeshkumar, *Resour. Eff. Technol.*, **3**, 406 (2017); https://doi.org/10.1016/j.reffit.2017.03.002
45. Y.A. Dallatu, G.A. Shallangwa and S.N. Africa, *J. Appl. Sci. Environ. Manag.*, **24**, 2147 (2021); https://doi.org/10.4314/jasem.v24i12.21
46. R. Sharma, R. Garg and A. Kumari, *EXCLI J.*, **19**, 1325 (2020); https://doi.org/10.17179/EXCLI2020-2842
47. A.N. Abraham, T.K. Sharma, V. Bansal and R. Shukla, *ACS Omega*, **3**, 2220 (2018); https://doi.org/10.1021/acsomega.7b01878
48. B.K. Sharma, B.R. Mehta, E.V. Shah, V.P. Chaudhari, D.R. Roy and S.M. Roy, *J. Cluster Sci.*, **33**, 2517 (2022); https://doi.org/10.1007/s10876-021-02145-x
49. S. Yedurkar, C. Maurya and P. Mahanwar, *Open J. Synth. Theory Appl.*, **5**, 1 (2016); https://doi.org/10.4236/ojsta.2016.51001
50. J. Vera, W. Herrera, E. Hermosilla, M. Díaz, J. Parada, A.B. Seabra, G. Tortella, H. Pesenti, G. Ciudad and O. Rubilar, *Antioxidants*, **12**, 784 (2023); https://doi.org/10.3390/antiox12040784
51. D.M. Sánchez-Pérez, E. Flores-Loyola, S.Y. Márquez-Guerrero, M. Galindo-Guzman and J.E. Marszalek, *Sustainability*, **15**, 3080 (2023); https://doi.org/10.3390/su15043080

52. M. Shiraz, H. Imtiaz, A. Azam and S. Hayat, *Biometals*, **37**, 23 (2024); https://doi.org/10.1007/s10534-023-00542-5
53. W. DeGroat, H. Abdelhalim, K. Patel, D. Mendhe, S. Zeeshan and Z. Ahmed, *Sci. Rep.*, **14**, 1 (2024); https://doi.org/10.1038/s41598-023-50600-8
54. J.A.A. Abdullah, A. Guerrero and A. Romero, *Appl. Sci.*, **14**, 1815 (2024); https://doi.org/10.3390/app14051815
55. H.K. Narendra Kumar, N.C. Mohana, B.R. Nuthan, K.P. Ramesha, D. Rakshith, N. Geetha and S. Satish, *SN Appl. Sci.*, **1**, 651 (2019); https://doi.org/10.1007/s42452-019-0671-5
56. E.P. Glaser, T.J. Kopper, W.M. Bailey, H.K. Kashif, R. Kumari, A.N. Stewart and J.C. Gensel, *Sci. Rep.*, **15**, 1 (2025); https://doi.org/10.1038/s41598-024-84936-6
57. T.L. Doane, C.H. Chuang, R.J. Hill and C. Burda, *Acc. Chem. Res.*, **45**, 317 (2012); https://doi.org/10.1021/ar200113c
58. S. Anjum, M. Inam, A.Y. Jassim, I. Attique, M. Zahra, F. Althobaiti, M.M. Soliman, K.S. Alotaibi, S.B. Albattal and C. Hano, *J. Taibah Univ. Sci.*, **19**, 2515712 (2025); https://doi.org/10.1080/16583655.2025.2515712
59. S. Pasieczna-Patkowska, M. Cichy and J. Flieger, *Molecules*, **30**, 684 (2025); https://doi.org/10.3390/molecules30030684
60. A. Jayachandran, A. T.R and A.S. Nair, *Biochem. Biophys. Rep.*, **26**, 100995 (2021); https://doi.org/10.1016/j.bbrep.2021.100995
61. M. Alekish, Z.B. Ismail, B. Albiss and S. Nawasrah, *Vet. World*, **11**, 1428 (2018); https://doi.org/10.14202/vetworld.2018.1428-1432
62. K. Punjabi, S. Mehta, R. Chavan, V. Chitalia, D. Deogharkar and S. Deshpande, *Front. Microbiol.*, **9**, 2207 (2018); https://doi.org/10.3389/fmicb.2018.02207
63. M.T. El-Saadony, G. Fang, S. Yan, S.S. Alkafaas, M.A. El Nasharty, S.A. Khedr, A.M. Hussien, S. Ghosh, M. Dladla, S.S. Elkafas, E.H. Ibrahim, H.M. Salem, W.F.A. Mosa, A.E. Ahmed, D.M. Mohammed, S.A. Korma, M.K. El-Tarabily, A.M. Saad, K.A. El-Tarabily and S.F. Abuqamar, *Int. J. Nanomedicine*, **19**, 12889 (2024); https://doi.org/10.2147/IJN.S487188
64. M. Banoee, S. Seif, Z.E. Nazari, P. Jafari-Fesharaki, H.R. Shahverdi, A. Moballegh, K.M. Moghaddam and A.R. Shahverdi, *J. Biomed. Mater. Res. B Appl. Biomater.*, **93**, 557 (2010); https://doi.org/10.1002/jbm.b.31615
65. S. Hamed and M. Emara, *Bratisl. Med. J.*, **126**, 2129 (2025); https://doi.org/10.1007/s44411-025-00223-4
66. S. Nasiri, H. Mahmoudvand, M. Shakibaei, S.A.H. Mousavi and A. Sepahvand, *J. Herbmed. Pharmacol.*, **11**, 540 (2022); https://doi.org/10.34172/jhp.2022.62
67. M.A. Abomuti, E.Y. Danish, A. Firoz, N. Hasan and M.A. Malik, *Biology*, **10**, 1075 (2021); https://doi.org/10.3390/biology10111075
68. M.T. Yassin, A.M. Elgorban, A.A. Al-Askar, E.N. Sholkamy, F. Ameen and K. Maniah, *Micromachines*, **14**, 209 (2023); https://doi.org/10.3390/mi14010209
69. M. Karkhane, H.E. Lashgarian, S.Z. Mirzaei, A. Ghaffarizadeh, K. Cherghipour, A. Sepahvand and A. Marzban, *Biocatal. Agric. Biotechnol.*, **29**, 101791 (2020); https://doi.org/10.1016/j.bcab.2020.101791
70. M. Abbas, A. Mumtaz, O.A. Mohammed, K. Zafar, I. Ahmed, M.T. Iqbal, M. Iqbal, A. Nazir, A.M.S. Eleragi, L.A. Saleh, M.A. Attia, E. Bahashwan, A.E.A.J. AlQahtani, S.M. Khan, W.A. El-Dakroury and A.S. Doghish, *J. Pharm. Innov.*, **20**, 112 (2025); https://doi.org/10.1007/s12247-025-10012-9
71. P. Kumar, A. Tapwal, S. Kumar and N. Thakur, *Adv. Nat. Sci. Nanosci. Nanotechnol.*, **15**, 025014 (2024); https://doi.org/10.1088/2043-6262/ad50bb
72. G. Marslin, K. Siram, Q. Maqbool, R.K. Selvakesavan, D. Kruszka, P. Kachlicki and G. Franklin, *Materials*, **11**, 940 (2018); https://doi.org/10.3390/ma11060940
73. M. Jiménez-Rosado, A. Gomez-Zavaglia, A. Guerrero and A. Romero, *J. Clean. Prod.*, **350**, 131541 (2022); https://doi.org/10.1016/j.jclepro.2022.131541
74. R. Javed, M. Usman, S. Tabassum and M. Zia, *Appl. Surf. Sci.*, **386**, 319 (2016); https://doi.org/10.1016/j.apsusc.2016.06.042
75. M. Ramakrishnan, R. Shanmugam, S. Neeharika, S. Selvaraj, J.J. Chokkattu and L. Thangavelu, *World J. Dent.*, **14**, 394 (2023); https://doi.org/10.5005/jp-journals-10015-2232
76. S.A. Al-Ghamdi, T.A. Alkathiri, A.E. Alfarraj, O.M. Alatawi, A.S. Alkathiri, C. Panneerselvam, S. Vanaraj, A.A.A. Darwish, T.A. Hamdalla, A. Pasha and S. Khasim, *Res. Chem. Intermed.*, **48**, 4769 (2022); https://doi.org/10.1007/s11164-022-04845-z
77. F. Eya, D.M. Murielle Nga Essama, E.L. Nguemfo, H.-D. Bamal, A. Antoinette Ntoumba, P. Belle Ebanda Kedi, T.H.Y. Beglau, A.K. Tako Djimefo, A.G. Djuidje, G.C. Tchatchouang, C. Christian Nanga, G.F. Nyuyfoni, A.F. Tchangou Njimou, D.I.M. Evouna, A.U.M. Fongang and C. Janiak, *bioRxiv*, 2024.12.15.628600 (2024); https://doi.org/10.1101/2024.12.15.628600
78. H. Agarwal and V.K. Shanmugam, *Bioorg. Chem.*, **94**, 103423 (2020); https://doi.org/10.1016/j.bioorg.2019.103423
79. O. Ragavan, M.N.H. Abdullah, L.Y. Fong, V. Lim and Y.K. Yong, *J. Cluster Sci.*, **35**, 2213 (2024); https://doi.org/10.1007/s10876-024-02681-2
80. R. Banchhor, A. Patel, M.K. Sharma, P. Ajazuddin, P. Jain, S.K. Gupta and K. Nagori, *Drug Deliv. Lett.*, **15**, (2025); https://doi.org/10.2174/0122103031350147250310032617
81. A.Q. Nkemzi, K. Okaiyeto, O. Oyenihi, C.S. Opuwari, O.E. Ekpo and O.O. Oguntibeju, *3 Biotech*, **14**, 291 (2024); https://doi.org/10.1007/s13205-024-04125-0
82. M. Azeem, M.H. Siddique, M. Imran, M. Zubair, R. Mumtaz, M. Younas, M.A. Abdel-Maksoud, M.A. El-Tayeb, M. Rizwan and J.W.H. Yong, *Heliyon*, **10**, e34073 (2024); https://doi.org/10.1016/j.heliyon.2024.e34073
83. K. Ramasubbu and V.D. Rajeswari, *Appl. Biochem. Biotechnol.*, **196**, 2652 (2024); https://doi.org/10.1007/s12010-023-04631-6
84. B. Padmavathy, B.S. Ebinezer, S. Amalraj, S. Kadaikunnan, M. Arumugam, V. Karthick, K. Karthikeyan, S. Prabhu, J.M. Khaled, J. Jose and R. Thiruvengadam, *Mater. Chem. Phys.*, **328**, 130030 (2024); https://doi.org/10.1016/j.matchemphys.2024.130030
85. S. Rajeshkumar, S.V. Kumar, A. Ramaiah, H. Agarwal, T. Lakshmi and S.M. Roopan, *Enzyme Microb. Technol.*, **117**, 91 (2018); https://doi.org/10.1016/j.enzmictec.2018.06.009
86. V. Sharma, D. Anderson and A. Dhawan, *Apoptosis*, **17**, 852 (2012); https://doi.org/10.1007/s10495-012-0705-6
87. D.P. Bai, X.F. Zhang, G.L. Zhang, Y.F. Huang and S. Gurunathan, *Int. J. Nanomedicine*, **12**, 6521 (2017); https://doi.org/10.2147/IJN.S140071
88. J. Stefanowicz-Hajduk, A. Hering, M. Kowalczyk, R. Hałasa, M. Gucwa and J.R. Ochocka, *Plants*, **12**, 2268 (2023); https://doi.org/10.3390/plants12122268